nature medicine

BRIEF COMMUNICATION

https://doi.org/10.1038/s41591-019-0343-4

Single-dose CRISPR–Cas9 therapy extends lifespan of mice with Hutchinson–Gilford progeria syndrome

Ergin Beyret[1,3], Hsin-Kai Liao[1,3], Mako Yamamoto[1,2], Reyna Hernandez-Benitez[1], Yunpeng Fu[1], Galina Erikson[1], Pradeep Reddy[1] and Juan Carlos Izpisua Belmonte[1*]

Hutchinson–Gilford progeria syndrome (HGPS) is a rare lethal genetic disorder characterized by symptoms reminiscent of accelerated aging. The major underlying genetic cause is a substitution mutation in the gene coding for lamin A, causing the production of a toxic isoform called progerin. Here we show that reduction of lamin A/progerin by a single-dose systemic administration of adeno-associated virus-delivered CRISPR–Cas9 components suppresses HGPS in a mouse model.

Laminopathies are degenerative disorders caused by mutations that affect proteins in the nuclear lamina[1]. The most severe forms manifest as accelerated aging at the organismal level in correlation with premature degeneration of multiple tissues and organs[2]. Therefore, these diseases are attractive platforms for identification of the molecular players of aging[3,4]. HGPS is one of the most severe forms of such diseases, with an early onset, fast progression and assured lethality[5,6]. It is diagnosed shortly after birth, and lethality ensues at an average age of 14.6 years[7]. No cure currently exists, and current treatments aim to alleviate the associated symptoms[8]. Although farnesyltransferase inhibitors have shown certain improvements and are now in clinical trials, this approach has limitations due to the potential side effects of these on other *CaaX* protein substrates, and because the effect of accumulated non-farnesylated progerin is unclear[9]. The majority of HGPS cases (~90%) result from a de novo c.C1824T (p.Gly608Gly) mutation that increases the usage of a cryptic splicing site and production of a truncated lamin A called progerin[10–12]. Truncation removes an endoproteolytic cleavage site, preventing removal of the farnesylated tail. Consequently, the nuclear envelope deforms and cellular functions associated with it are impaired, including genomic stability, epigenetic regulation of gene expression, protein and energy metabolism and nucleocytoplasmic transport[3,4,6,13]. Induction of the corresponding mutation in the mouse (Gly609Gly) induces phenotypes similar to those in human patients[14]. On the other hand, lamin A appears to be dispensable, possibly due to compensation from its shorter isoform, lamin C[14,15], and mice without lamin A live longer than wild-type (WT) mice[16], indicating that HGPS results not from lack of lamin A but from the accumulation of progerin. Therefore, we reasoned that HGPS can be treated by CRISPR–Cas9-targeted disruption of lamin A/progerin.

Two guide RNAs (gRNAs; gLmna-1 and gLmna-2) for *Streptococcus pyogenes* Cas9 targeting lamin A downstream of lamin C were designed to reduce lamin A/progerin without perturbing lamin C (Fig. 1a). The efficiency of the targeting was evaluated in fibroblasts isolated from HGPS-Cas9 mice that are heterozygous or homozygous for the progerin mutation and hemizygous for a constitutively active Cas9 transgene. Lentiviral delivery of the gRNAs individually or together efficiently downregulated the levels of progerin and lamin A but not that of lamin C (Extended Data Fig. 1a,b). Neither a gRNA with no target site on the genome (mock-treatment) nor the gRNAs without Cas9 elicited the effect, indicating that downregulation results from lamin A/progerin targeting by CRISPR–Cas9. Interestingly, high-throughput RNA sequencing showed that both gRNA treatments correlated with downregulation of the RNA sequences downstream of lamin C, suggesting that these treatments resulted in either lamin A/progerin-specific transcriptional interference or RNA destabilization (Extended Data Fig. 1c,d). A similar concurrent study[17] and a previous knock-in attempt in this region also came to the same conclusion[15].

We next tested the in vivo efficacy of gRNAs in HGPS-Cas9 mice. Toward this end, individual gRNAs with a mCherry reporter were packaged into adeno-associated virus (AAV) with serotype 9 (AAV9). Given that HGPS is a pediatric systemic disease, we systemically delivered AAV9-gRNAs into neonatal mice via facial vein injection (Fig. 1b). Both gRNAs were collectively administered for maximum efficiency (gLmna-1 + gLmna-2). mCherry reporter was detectable on day 4 post-injection in several organs, with liver displaying the highest expression (Fig. 1b,c and Extended Data Fig. 2a). The distribution of mCherry expression among organs remained the same throughout adulthood, except for the intestine, in which it was reduced to the background level (Extended Data Fig. 2b,c). Genomic DNA isolated from the organs of adult mice injected with gRNA showed the highest level of editing in the liver in correlation with protein levels (Fig. 1d,e and Extended Data Fig. 3). Consequently, the mice looked healthier and displayed an improved posture and body weight (Fig. 1f,g). Moreover, they were more active, which may have been due to systemic physiological improvement and suppression of kyphosis (Supplementary Videos 1 and 2).

HGPS mice fail to thrive and gradually lose body weight with age[14]. We monitored the body weight progression of the treated mice in comparison to negative controls from 2 months of age. We observed that treatment attenuated weight loss (Fig. 2a). In parallel, the median survival rate increased by approximately 25% (Fig. 2b). The median survival rates for HGPS, HGPS-Cas9 and HGPS-Cas9 + two Lmna-gRNAs (g1&2) mice were 16.7, 20.0 and 25.3 weeks, respectively. Given that HGPS is a progressive degenerative disorder, we analyzed gastric and dermatological histology.

[1]Salk Institute for Biological Studies, La Jolla, CA, USA. [2]Universidad Católica San Antonio de Murcia , Murcia, Spain. [3]These authors contributed equally: Ergin Beyret, Hsin-Kai Liao. *e-mail: belmonte@salk.edu

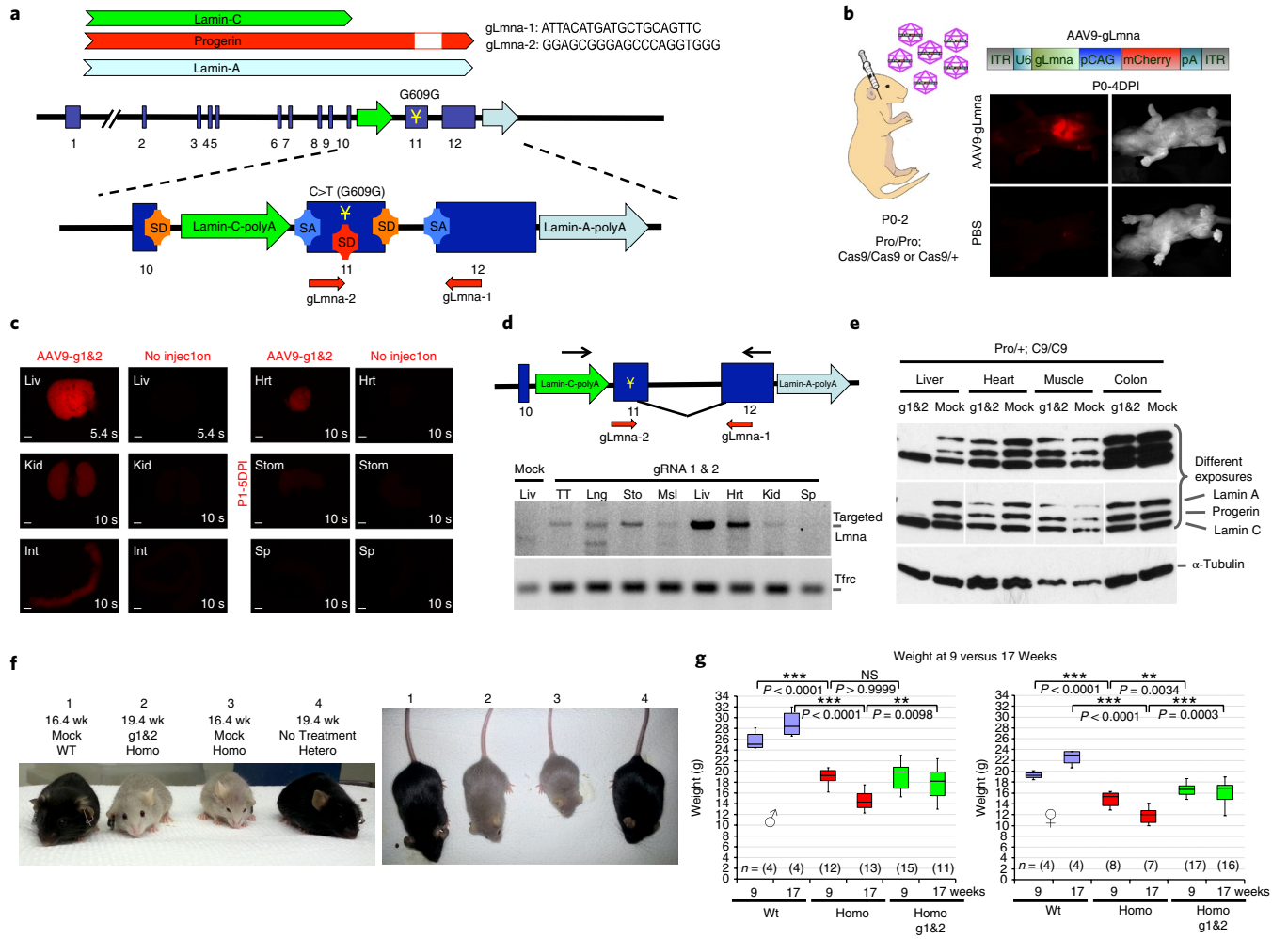

Fig. 1 | Targeted disruption of lamin A and progerin by CRISPR–Cas9. a, Scheme of lamin A/progerin targeting by CRISPR–Cas9. gLmna-1 targets upstream of the farnesylation site, while gLmna-2 recognizes mutation and the WT site (Y). SA: splice activator site; SD: splice donor site. **b**, The in vivo gene therapy scheme. AAV9-mCherry-gLmna was injected into 0- to 2-day-old mice (P0-2). Upper panels show the mCherry signal 4 days post-injection (DPI) of a P0 mouse (P0-4DPI) versus the PBS-injected control (lower panels). **c**, Expression of the mCherry reporter in different organs at 6 d postpartum (P1-5DPI). The numbers at the lower right corners denote the exposure time. Scale bar, 2 mm. **d**, Efficiency of lamin A/progerin targeting. When both gRNAs act simultaneously, the region between them is deleted and the re-ligated ends can be detected by PCR. Black arrows denote the location of the primers. Tfrc: positive control for PCR; Mock: a gRNA with no target site on the genome. **e**, Immunoblots of adult organ lysates from heterozygous HGPS (Pro/+) mice on homozygous Cas9 (C9/C9) background treated with g1&2 versus mock-treated to evaluate lamin A/C/progerin levels. Middle panel corresponds to the uppermost blot under different exposures. α-Tubulin: loading control (Fig. 1b–e shows representative replicates of at least two independent experiments). **f**, Gross mouse morphology. Shown are 16.4-week-old (wk) mock-treated WT and homozygous (homo) female siblings next to 19.4-week-old heterozygous (hetero) and g1&2-treated homozygous female siblings (also shown in Supplementary Videos 1 and 2). The difference in morphology occurs because the mock-treated controls are 3 weeks younger. **g**, Body weight comparison between mice at 9 and 17 weeks of age, with data from males in the left panel and from females in the right. In each box plot, the box extends from the 25th and 75th percentiles, and the black line in the middle represents the median. The whiskers show the upper and lower limits of the data. Significance was determined by one-way ANOVA with Bonferroni correction. Liv, TT, Hrt, Lng, Kid, Stom, Msl, Int, Sp: liver, tail tip, heart, lung, kidney, stomach, muscle, intestine, spleen, respectively.

These two organs undergo accelerated aging in HGPS mice[18], although human patients with HGPS do not demonstrate clinically impaired gastrointestinal function. The treated mice displayed a qualitatively healthier glandular stomach, with the number of parietal cells comparable to WT control, while the mock-treated mice were notably deficient in parietal cells. The treatment also suppressed epidermal thinning and dermal fat loss, two aging-associated skin conditions (Fig. 2c,d).

Because death in patients with HGPS is due mainly to cardiovascular ailments similar to those seen in old age, we investigated the aortic arch and heart rate in HGPS mice. Treatment ameliorated the degeneration of vascular smooth muscle cells of the aortic arch compared to control mice, as indicated by an increase in the number of nuclei in the medial layer (Extended Data Fig. 4a). Furthermore, although human patients with HGPS do not demonstrate decreased heart rates, electrocardiographic analysis in HGPS mice revealed that treatment attenuated the development of bradycardia (Extended Data Fig. 4b).

The musculoskeletal system is one of the major systems impaired during aging and in HGPS, affecting the quality of life. We assessed musculoskeletal physiology by subjecting mice to the grip strength test. The treated mice exhibited stronger forelimb and hindlimb

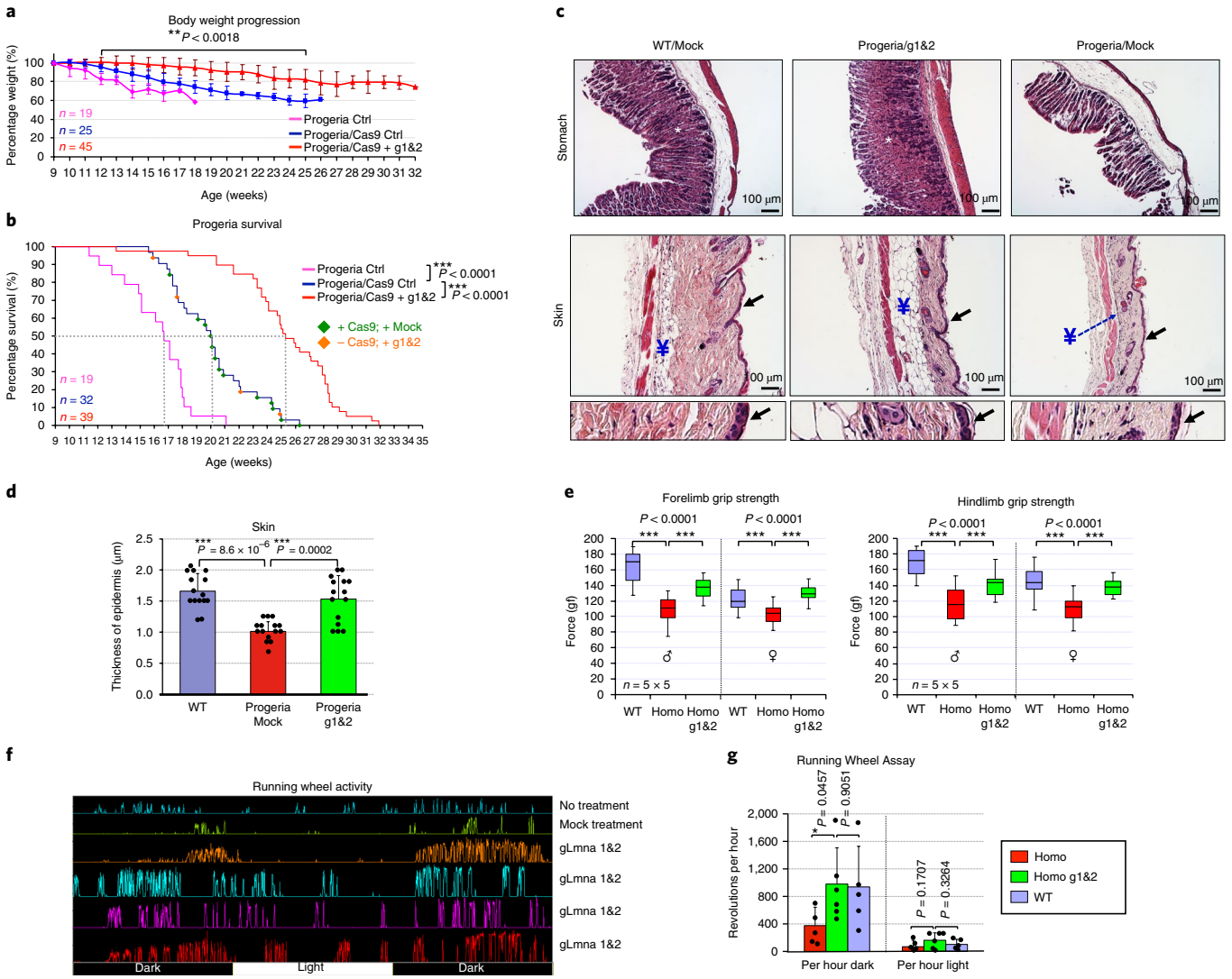

Fig. 2 | CRISPR–Cas9-induced reduction of lamin A/progerin enhances the health and extends the lifespan of HGPS mice. a,**b**, Body weight (**a**) and survival rates (**b**) over time. The magenta line denotes untreated homozygous HGPS (Progeria) mice according to Ocampo et al.[18]. The blue and red lines denote mice developed by crossing HGPS and Cas9 transgenic mice (Progeria/Cas9 mice). These are homozygous for HGPS and carry at least one copy of the Cas9 transgene (hemi- or homozygous). The blue line in **b** denotes unedited mice, including untreated, mock-treated (green diamond) and gRNA-only (orange diamond) negative controls. The red line denotes g1&2-treated mice. The sample size (*n*) indicates the initial number of mice at week 9. Shown are mean values ± s.d. Multiple *t*-tests and log-rank (Mantel–Cox) were used for body weight and survival curves, respectively. Although introduction of Cas9 alone appeared to increase the survival rate, this may have resulted from the different strain backgrounds following crossing with Cas9 mice. **c**, Histological analyses comparing stomach (upper panels) and skin (lower panels) derived from 19-week-old g1&2-treated versus mock-treated homozygous mice next to mock-treated WT. The arrows and asterisks denote epidermal and gastric parietal cells, respectively. ¥: dermal fat. The figures at the bottom are enlarged views of epidermal regions indicated by the arrows. The images are representative replicates of two independent experiments with similar results. Scale bar, 100 μm. **d**, Measurement of epidermal thickness (*n* = 15 sections per group from three biologically independent samples). Mean, s.e.m. and statistical significance according to unpaired Student's *t*-test. **e**, Grip strength test. Left and right panels depict forelimb and hindlimb grip strength (gf, grams of force) of adult mice (16–18 weeks old), respectively. Each estimate corresponds to 25 reads derived from five animals, measured five times. In each box plot, the box extends from the 25th and 75th percentiles, and black lines in the middle represent the median. The whiskers show the upper and lower limits of the data. Significance was determined by one-way ANOVA with Bonferroni correction. **f**, Representative graph of running wheel activities. Shown are the activities of untreated or mock-treated versus four g1&2-treated homozygous mice. All the mice were 17 weeks old, except no treatment control was 13 weeks old. **g**, Quantitation of running wheel activities. Mice tested were 10–18 weeks of age. Blue bars denote WT mice (*n* = 5) while red and green bars denote control (*n* = 5) and g1&2-treated (*n* = 6) homozygous HGPS mice, respectively. Shown are mean values ± s.d. and significance according to unpaired *t*-tests.

grip in parallel with higher body weight. Given that there are no neurological deficits in HGPS, this observation indicates that the physiological decline in skeletal muscle is suppressed (Fig. 2e and Extended Data Fig. 4c). We next evaluated the vitality of the mice by measuring their voluntary activity on a running wheel. The treated mice retained their activity at a level similar to WT controls (Fig. 2f,g). These results indicate that targeting of lamin A/progerin by CRISPR–Cas9 in HGPS mice improved their physiological functions in correlation with histological improvements, and extended their life expectancy.

Despite the increased survival rate observed, the lifespan of treated mice was less than that of WT. We observed that a significant number of treated mice died suddenly, unlike the progressive deterioration seen in untreated mice (Extended Data Fig. 5a). Before death, treated mice displayed acute weight loss and abdominal distension, in parallel with difficulty in defecation (Extended Data Fig. 5b). Necropsy findings indicated the presence of megacolon/megacecum alongside hardened fecal matter, suggesting that the reason for the sudden lethality observed was inability to discharge excrement (Extended Data Fig. 5c). Given that lamin C-only transgenic mice are asymptomatic[14] whereas accumulation of farnesylated lamin A in the enteric nervous system induces the same symptoms[19], our observations suggest that the lethality observed may have been due to failure of the colonic nervous system resulting from the absence of gene editing (Fig. 1e). Neither untreated nor mock-treated mice developed this phenotype, presumably because they had died beforehand.

Altogether, our data show that CRISPR–Cas9-mediated lamin A/progerin reduction by single intravenous injection enhanced the health and extended the lifespan of HGPS mice. In this study, we used transgenic mice that express *S. pyogenes* Cas9 and exogenously deliver gRNAs as a proof of concept. Notably, the accompanying paper by Santiago-Fernández et al.[17] demonstrates similar conclusions following intraperitoneal delivery of *Staphylococcus aureus* Cas9 and gRNAs[17]. These two independent studies are therefore complementary and reveal the potential use of CRISPR–Cas9 in the treatment of human patients with HGPS. Although this strategy perturbs lamin A expression alongside progerin expression, knockout studies in mice show that individuals lacking lamin A are viable[14–16] and even live longer than WT mice[16]. Given that HGPS is a lethal disorder, the improvement in health and extended lifespan achieved by this approach offers an attractive mode of intervention. Interestingly, although we observed a modest therapeutic effect, this outcome correlated with the occurrence of gene editing occurring mainly in the liver and minimally in other organs. A more wide-spectrum targeting, including the colon or combination therapy with farnesyltransferase inhibitors[9], may further serve to extend the life expectancy of patients with HGPS.

Online content

Any methods, additional references, Nature Research reporting summaries, source data, statements of data availability and associated accession codes are available at https://doi.org/10.1038/s41591-019-0343-4.

Received: 22 January 2018; Accepted: 21 December 2018;
Published online: 18 February 2019

References

1. Worman, H. J., Fong, L. G., Muchir, A. & Young, S. G. *J. Clin. Invest.* **119**, 1825–1836 (2009).
2. Broers, J. L., Ramaekers, F. C., Bonne, G., Yaou, R. B. & Hutchison, C. J. *Physiol. Rev.* **86**, 967–1008 (2006).
3. Kubben, N. & Misteli, T. *Nat. Rev. Mol. Cell Biol.* **18**, 595–609 (2017).
4. Gordon, L. B., Rothman, F. G., Lopez-Otin, C. & Misteli, T. *Cell* **156**, 400–407 (2014).
5. Ahmed, M. S., Ikram, S., Bibi, N. & Mir, A. *Mol. Neurobiol.* **55**, 4417–4427 (2018).
6. Gonzalo, S., Kreienkamp, R. & Askjaer, P. *Ageing Res. Rev.* **33**, 18–29 (2017).
7. Gordon, L. B. et al. *Circulation* **130**, 27–34 (2014).
8. Gordon, L. B. et al. *GeneReviews® [Internet]* (NCBI Bookshelf, 2003).
9. Young, S. G., Yang, S. H., Davies, B. S., Jung, H. J. & Fong, L. G. *Sci .Transl. Med.* **5**, 171ps3 (2013).
10. Vidak, S. & Foisner, R. *Histochem. Cell. Biol.* **145**, 401–417 (2016).
11. De Sandre-Giovannoli, A. et al. *Science* **300**, 2055 (2003).
12. Eriksson, M. et al. *Nature* **423**, 293–298 (2003).
13. Buchwalter, A. & Hetzer, M. W. *Nat. Commun.* **8**, 328 (2017).
14. Osorio, F. G. et al. *Sci. Transl. Med.* **3**, 106ra107 (2011).
15. Fong, L. G. et al. *J. Clin. Invest.* **116**, 743–752 (2006).
16. Lopez-Mejia, I. C. et al. *EMBO Rep.* **15**, 529–539 (2014).
17. Olaya Santiago-Fernández, F. G. O. et al. *Nat. Med.* (in the press).
18. Ocampo, A. et al. *Cell* **167**, 1719–1733 e12 (2016).
19. Yang, S. H. et al. *Hum. Mol. Genet.* **24**, 2826–2840 (2015).

Acknowledgements

We thank A. Ocampo for discussions throughout the study and M. Schwarz for administrative support. We are grateful to G. Sancar and Ronald Evans Lab for providing the running wheel equipment. E.B. was partially funded by the Catharina Foundation. P.R. was partially supported by the Muscular Dystrophy Association. G.E. was partially funded by NIH-NCI CCSG: P30 014195 and by the Helmsley Trust. Work in the laboratory of J.C.I.B. was supported by The Progeria Research Foundation, Universidad Católica San Antonio de Murcia (UCAM), Fundacion Dr. Pedro Guillen, the G. Harold and Leila Y. Mathers Charitable Foundation, The Glenn Foundation and The Moxie Foundation.

Author contributions

E.B., H.-K.L. and J.C.I.B. designed all the experiments. E.B., H.-K.L., P.R. and J.C.I.B. prepared the figures and wrote the manuscript. E.B., H.-K.L. and Y.F. performed and/or analyzed in vitro experiments. E.B., H.-K.L., Y.F., M.Y., R.H.-B. and P.R. performed and/or analyzed ex vivo and in vivo experiments. G.E. performed the bioinformatics analyses.

Competing interests

The authors declare no competing interests.

Additional information

Extended data is available for this paper at https://doi.org/10.1038/s41591-019-0343-4.

Supplementary information is available for this paper at https://doi.org/10.1038/s41591-019-0343-4.

Reprints and permissions information is available at www.nature.com/reprints.

Correspondence and requests for materials should be addressed to J.C.I.

Publisher's note: Springer Nature remains neutral with regard to jurisdictional claims in published maps and institutional affiliations.

Methods

All animal procedures were performed according to National Institutes of Health guidelines and were approved by the Committee on Animal Care at the Salk Institute.

Mouse strains. The HGPS (Progeria) mouse model, carrying the progerin mutation G609G, was generated by C. López-Otín at the University of Oviedo, Spain and was kindly donated by B. Kennedy of the Buck Institute. *Streptococcus pyogenes* Cas9 transgenic mice were obtained from Jackson Laboratory (stock No: 024858). HGPS mice are a cross between strains 129/Ola and C57BL/6, and Cas9 mice have a background of 129, C57BL/6N, C57BL/6J and FVB/N. Homozygous Progeria mice are infertile. Heterozygous mice were crossed with homozygous Cas9 mice to obtain the composite mice. The resulting trans-heterozygous mice were bred to obtain the homozygous Progeria mice that carry the Cas9 transgene (homo- or hemizygous). The hemizygous Cas9 background was sufficient to reduce Lamin A/progerin levels (Extended Data Fig. 3b). Heterozygous Progeria mice with the Cas9 background were used to maintain the line. Progeria mice are strain C57BL/6, while Cas9 mice have a mixed background of 129, C57BL/6 and FVB/N. Mice were housed with a 12-h light/dark cycle between 06:00 and 18:00 in a temperature-controlled room (22 ± 1 °C) with free access to water valves and PicoLab Rodent Diet 20 (LabDiet, catalog No: 5053) provided on a wire bar lid. Mice that had lost >20% weight within 1 week or those whose body weight fell below 13 g were provided moist food on the cage floor and a water bottle on the wire bar lid.

gRNA design. gLmna-1 was designed to target exon 12 of the mouse gene lamin A, and encompasses the farnesylation site. gLmna-2 was designed to target exon 11 in close proximity to the C > T HGPS mutation site. A gRNA with no target site on the genome was used as the mock-gRNA control (gRNA Mock). gRNA sequences are listed in Supplementary Table 1.

In vivo LMNA gene therapy. Individual gRNAs were packaged into AAV9 vectors with the mCherry reporter according to a published protocol[20]. Expression of the gRNA and mCherry was driven by U6 and CAG promoters, respectively. A 1:1 mix of AAV9-gRNA1 and -gRNA2 was injected in 40 µl phosphate buffered saline (PBS) into the facial vein of neonatal mice under hypothermia-induced anesthesia within 48 h of birth (P0-2). Mice infected with AAV9s carrying mCherry alongside a gRNA with no target on the genome (Mock), or mCherry alone, were used as negative controls in addition to the untreated mice (no gRNA). Likewise, mice without the Cas9 transgene that underwent AAV9-gRNA1&2 treatment served as the 'no Cas9' control. All negative controls displayed similarly. The injected titre ranged between 2×10^{10} and 1×10^{12} genomic copies (gc) per gRNA virus as determined by quantitative PCR: 2.6×10^{10} gc total (Fig. 1b), 2.6×10^{11} gc each (Fig. 1c), 1.2×10^{11} gc each (Fig. 1d), 4.8×10^{11} gc each (Fig. 1e), 6.2×10^{10} gc each (Fig. 1f), 6.2×10^{10} gc each (Fig. 2c). Detection of the mCherry signal was obtained with a Zeiss AxioZoom.V16 stereoscopic microscope. Adult mice were perfused with PBS to wash out blood before the organs were extracted for imaging.

For the genomic DNA analysis shown in Fig. 1d, post-mortem tissues were first digested with 1 mg ml^{-1} Proteinase K in 100 mM NaCl, 25 mM ethylenediaminetetraacetic acid, 10 mM Tris pH 8.0 and 0.5% sodium dodecyl sulfate overnight at 55 °C. Genomic DNA from the digests was isolated with phenol:chloroform:isoamyl alcohol (25:24:1) extraction followed by ethanol precipitation. DNA was digested with HindIII (New England Biolabs, catalog no: R0104) to remove non-truncated lamin A, to enhance PCR amplification of lamin A that had undergone truncation by the simultaneous cleavages of gRNA1 and 2.

For analysis of protein levels by immunoblotting, organs were isolated from mice perfused with PBS and homogenized in RIPA buffer (50 mM Tris-HCl pH7.4, 150 mM NaCl, 2 mM ethylenediaminetetraacetic acid, 1% NP-40, 0.1% sodium dodecyl sulfate, 0.5% sodium deoxycholate, 1 mM phenylmethanesulfonyl fluoride and ×1 Mini Protease inhibitor cocktail (Roche, catalog No: 11836153001)). Genomic DNA was sheared by passing the lysate ten times through a 23 G needle. After 30 min incubation on ice, the lysate was centrifuged at 13,000 relative centrifugal force at 4 °C for 5 min to remove debris. The protein concentration was estimated witha BCA Protein Assay Kit (Pierce, catalog Nos: 23225 and 23227). The lysate was then supplemented with 1 mM dithiothreitol before running 5–25 µg total protein on a 10–20% Novex WedgeWell Tris-Glycine gel (catalog No: XP1020-Box). Immunoblotting was performed on 0.45-µm polyvinylidene difluoride membranes. The membranes were blocked with 5% nonfat dry milk powder in Tris-buffered saline with 0.1% Tween 20 for 20 min at room temperature. Immunoblotting with primary and secondary antibodies was performed for either 2 h at room temperature or overnight at 4 °C. Detection was performed using either SuperSignal West Pico or Femto Chemiluminescence Substrate Solution (ThermoFisher Scientific, catalog Nos: 34087 and 34095) on Hyblot CL autoradiography film (catalog No: E3018). The membranes were stripped by incubation in Restore Plus Stripping Buffer (ThermoFisher Scientific, catalog No: 46428) for 15 min at room temperature for re-probing. Immunoblotting was repeated at least twice with different samples (biological replicates). Full-length images of the immunoblots are provided in the Source Data, and quantification of bands was performed by ImageJ software based on their integrated densities per area.

Ex vivo LMNA gene therapy. Primary fibroblasts were isolated from the tail tips of adult mice of the indicated genotypes. A total of 45,000 cells were seeded per well of a 12-well plate the day before they were infected with lentivirus expressing the mCherry reporter and the individual gRNA-Lmna-1 and -2 or mock-gRNA. mCherry-positive cells in the culture were visually counted microscopically in at least three visual fields to estimate infectivity, where >65% infectivity was observed. No selection or cell sorting was performed following infection. The cells were passaged at least once before lysing for immunoblotting. These were processed for immunoblotting using the same method used for tissue samples, except that sodium deoxycholate was not included in the RIPA buffer used for lysis.

Histological analyses. For the histological analyses, 19-week-old mice of the indicated genotypes were perfused first with PBS then with 10% formalin; the exception was aortic arch samples, where 4% paraformaldehyde was used rather than formalin. Whole organs were incubated in 10% formalin at room temperature for 2 d; aortic arch tissues were incubated in 4% paraformaldehyde at 4 °C for 16 h. All samples were stored in 70% ethanol at 4 °C until required for paraffin embedding and sectioning. Sections were analyzed with H&E staining. Calculation of the area of medial layers and the number of nuclei they contained was done using ImageJ 1.52c software, with between three and five mice under each condition being analyzed. The total number of slide sections used for quantitation is indicated in the corresponding Figure legends.

Physiological analyses. For analysis of the heart rate, mice were anesthetized with 2.5% isoflurane and monitored using the Power Lab data acquisition instrument (ADInstruments). Data processing and analysis were performed using LabChart8 (ADInstruments).

For the grip strength test, a tension meter measuring force in Newtons was stationed horizontally on a platform. The mouse was held by the tail and allowed to grip the tension bar with both paws before being pulled slowly away from the bar until its grip was broken. Five adult female mice and five adult male mice (16–18 weeks old) were used for each group (WT, treated homozygous Progeria and negative control). Each mouse was subjected to the test five times each for forelimb and hindlimb strength. Each estimate given corresponds to 25 reads derived from five animals, measured five times.

Activity on the voluntary running wheel was recorded with low-profile wireless running wheels connected to a computer via a wireless hub, and analyzed using the dedicated software (Med Associates Inc., catalog No: ENV-047). The animals were allowed to adapt to the apparatus for at least 22 h before their activities were input to the estimation; acceptable adjustment was considered to have been attained as determined by their activities showing circadian correlation (i.e., active at night). One of the 27 mice analyzed showed no interest in this activity, as determined by small sporadic peaks of activity with no circadian correlation; this mouse was therefore excluded from the study. All mice showing even a low level of activity but with circadian correlation were included.

DNA library preparation and deep sequencing. Nested PCR was performed for the preparation of DNA libraries for deep sequencing. The Lmna F and Lmna R primers shown in Fig. 1d were also included in this procedure. These were used for the first round of amplification of the nested-PCR procedure with limited PCR cycles using 100 ng of genomic DNA. This PCR product was used for the second round of amplification in the nested-PCR procedure using primer pairs containing adaptor sequences for deep sequencing (Lmna-1-adapter-F1 and Lmna-1-adaptor-R1 or Lmna-2-adapter-F3 and Lmna-2-adaptor-R3). The nested-PCR product was purified using the QIAquick PCR Purification Kit (QIAGEN). This cleaned DNA library preparation was subjected to deep sequencing as in the published protocol[19]. Primer sequences are listed in Supplementary Table 1.

RNA-sequencing analyses. Total RNA was isolated from the primary tail tip fibroblasts of the indicated genotypes and treatments. gRNAs were delivered into the cultured cells by lentiviral vectors. The cells were homogenized with Qiashredder spin columns (QIAGEN) and processed with the RNeasy Mini Kit (QIAGEN) for isolation of total RNA. Quality assessment, library construction and sequencing (stranded messenger RNA, HiSeq SE50) were performed by the Next Generation Sequencing Core of Helmsley Center for Genomic Medicine at Salk Institute. Bioinformatics analyses were performed by the Razavi Newman Integrative Genomics and Bioinformatics Core at Salk Institute. Sequenced reads were quality tested using FASTQC and aligned to the mm10 mouse genome using STAR[21] version 2.5.1b. Mapping was performed using the default parameters (up to ten mismatches and up to nine multi-mapping locations per read). The normalized fragments per kilobase per million mapped reads were quantified across all annotated exons. Normalized read densities were visualized using the University of California, Santa Cruz genome browser.

Antibodies. The following antibodies were used for immunoblotting at the indicated dilutions: Anti-LAMIN A/C (N-18) 1:100 (SantaCruz, catalog No:

sc6215), Anti-LAMIN A/C (E-1) 1:100 (SantaCruz, catalog No: sc376248), anti-β actin 1: 600 (SantaCruz, catalog No: sc47778) and anti-α-tubulin 1: 750 (Calbiochem, catalog No: CP06). Horseradish peroxidase-conjugated secondary antibodies were anti-goat 1:500 (Novex, catalog No: A15909) and anti-mouse 1:1,000 (Cell Signaling, catalog No: 7076)

Statistical analyses. Average (mean), s.e.m. and statistical significance were calculated by unpaired Student's *t*-test (Fig. 2g), multiple *t*-test (Fig. 2a) or one-way ANOVA with Bonferroni correction (Figs. 1g and 2e) and log-rank (Mantel–Cox) test (Fig. 2b) using Microsoft Excel or GraphPad Prism. $P < 0.05$ was considered significant ($^{*}P < 0.05$, $^{**}P < 0.01$, $^{***}P < 0.001$), $P \geq 0.05$ were denoted as statistically not significant (NS).

Reporting Summary. Further information on research design is available in the Nature Research Reporting Summary linked to this article.

Data availability

The accession number for the RNA-Seq data reported in this paper is NCBI GEO: GSE122865.

References

20. Liao, H. K. et al. *Cell* **171**, 1495–1507 e15 (2017).
21. Dobin, A. et al. *Bioinformatics* **29**, 15–21 (2013).

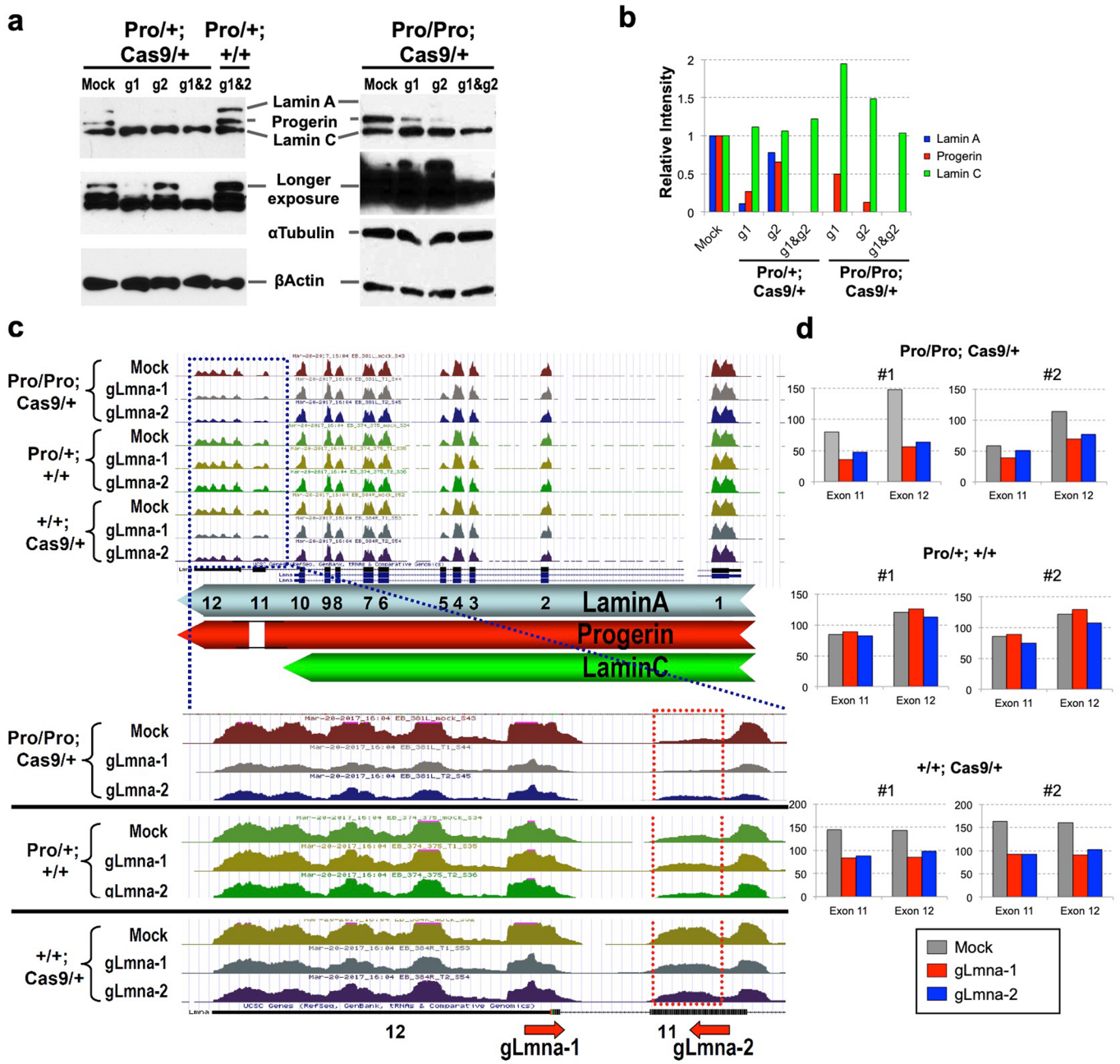

Extended Data Fig. 1 | Immunoblots and RNA sequencing of Lmna gRNA-treated fibroblasts of adult HGPS mice. a, Immunoblots of individual (g1 or g2) or multiplex (g1&2) gRNA-treated fibroblasts derived from adult HGPS (Pro); Cas9 mice. Fibroblasts derived from heterozygous (Pro/+) and homozygous (Pro/Pro) HGPS mice of a heterozygous Cas9 (Cas9/+) background were treated with lentivirally delivered gRNAs. No Cas9 (Pro/+;+/+) sample or mock-treatments were used as negative controls. Middle panels show longer exposures. α-Tubulin and β-actin were used as loading controls. **b**, Relative intensities of lamin A, progerin and lamin C bands on the immunoblots. The intensity of each band was normalized by β-actin intensity and compared to normalized mock-control. **c**, Custom tracks of RNA sequences identified with high-throughput sequencing. The magnified region corresponds to the square blue area. The red line denotes the truncated region in HGPS (Pro). Shown are RNA samples derived from mouse fibroblasts of the indicated genotypes and treatments: + denotes WT. Mock-treatments and heterozygous HGPS mice without Cas9 (Pro/+; +/+) were used as negative controls. The arrows are not drawn to scale. **d**, Quantification of RNA sequencing analyses shows reduced transcription of exons 11 and 12 in Cas9-positive cells treated with gRNAs relative to mock-treated or Cas9-negative cells.

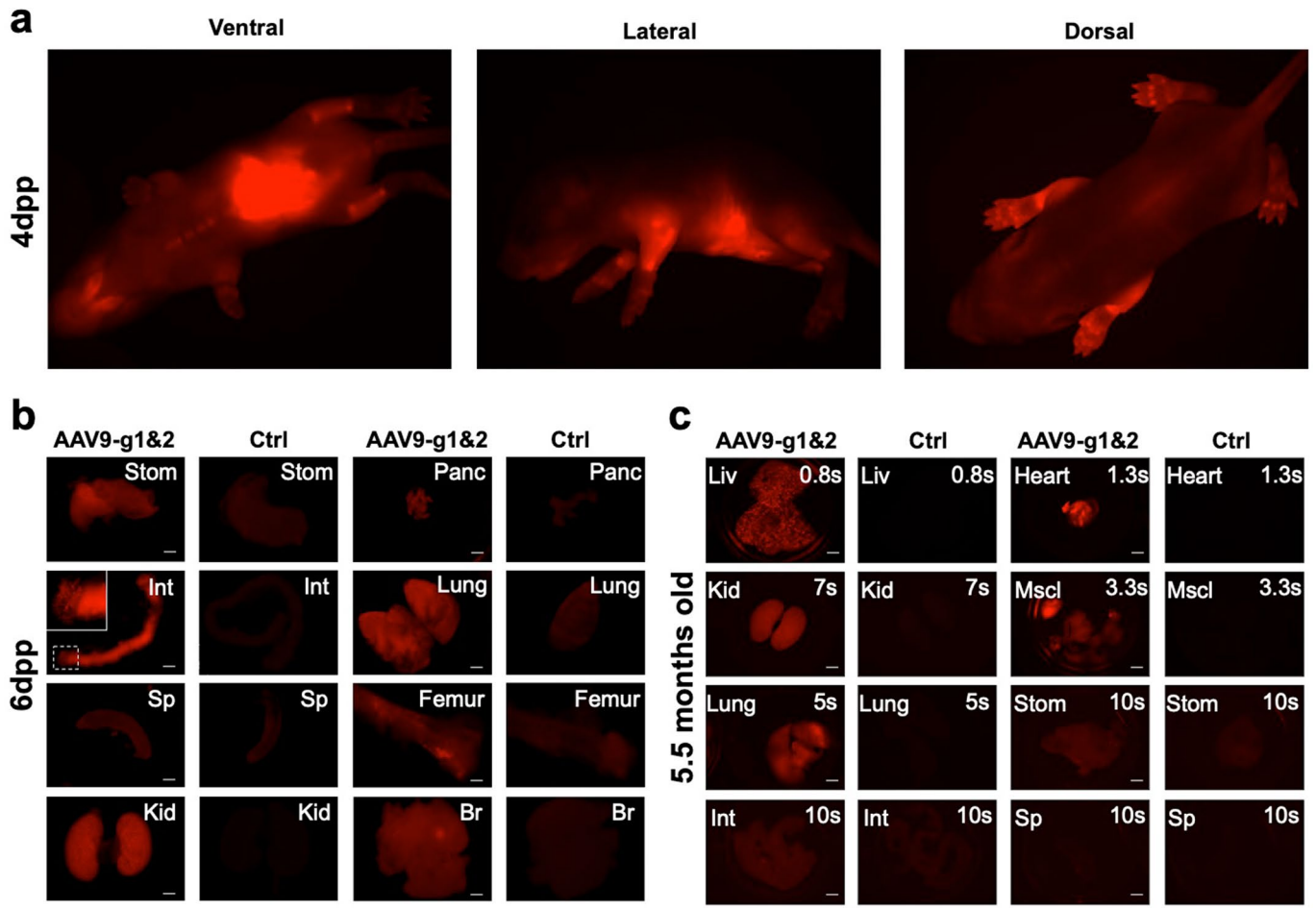

Extended Data Fig. 2 | Fluorescent images of Lmna gRNA-injected mice. a, Whole-body fluorescent images of a P4 (4 days dpp, days postpartum) mouse injected at P0 with a 1:1 mix of gRNA1 and gRNA2 viral preparations (each 1.29×10^{11} genomic copies per viral preparation). **b**, Same organs as in Fig. 1c, under individually adjusted exposure levels relative to negative controls. The organs were harvested from a 6 dpp mouse, 5 days post-injection (dpi) at P1 (P1-5DPI). The inset corresponds to the square area. Ctrl: no injection. **c**, Expression of the mCherry reporter in the adult (5.5 months post-injection of a 1:1 mix of gRNA1 and 2 viral preparations;1.3×10^{11} genomic copies per viral preparation). The numbers at the upper right corner denote the exposure times. stom, panc, int, sp, kid, br, liv, mscl: stomach, pancreas, intestine, spleen, kidney, brain, liver, muscle, respectively.

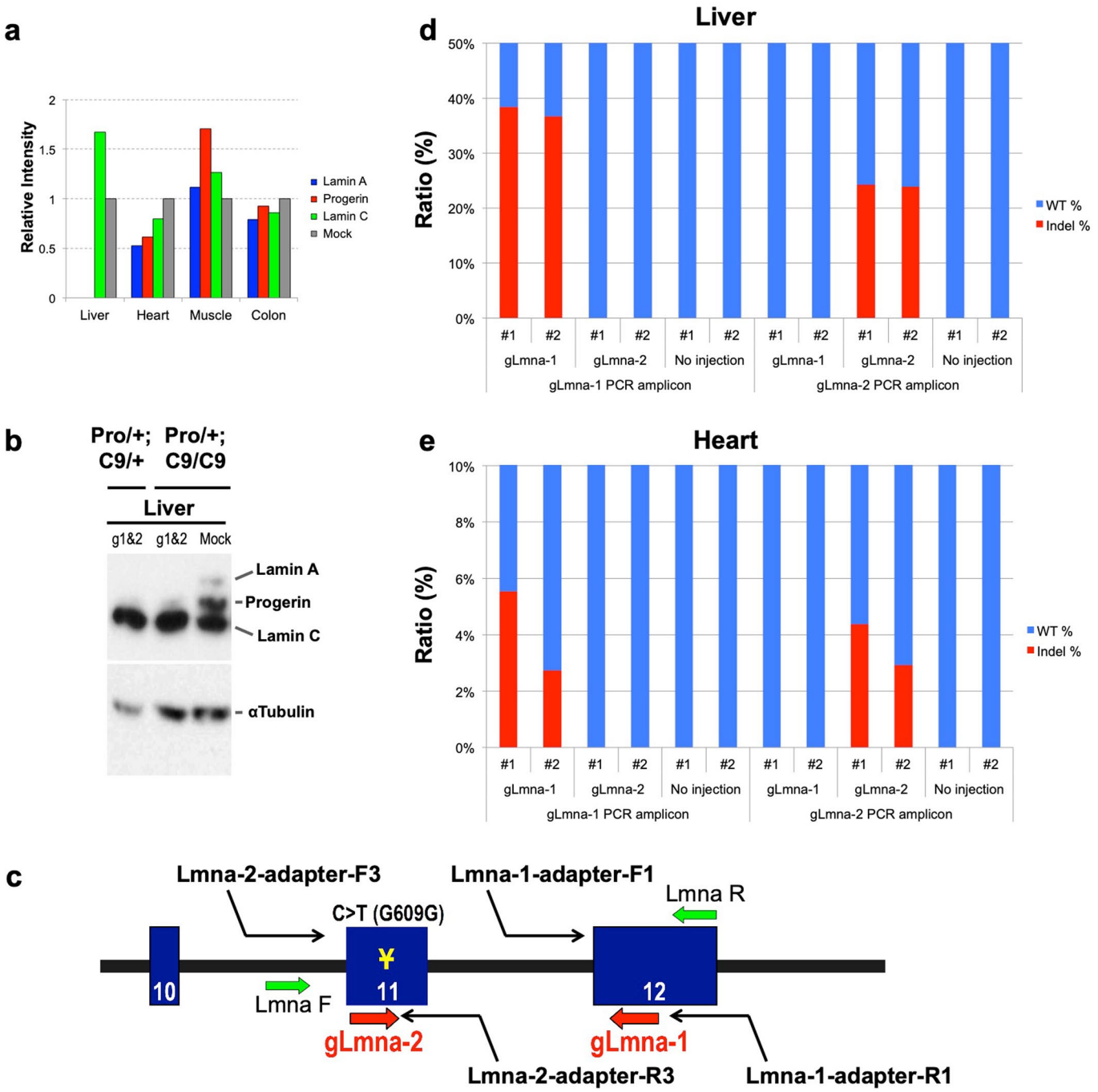

Extended Data Fig. 3 | Genomic DNA and protein analyses of Lmna gRNA-treated mice. a, Relative intensities of lamin A, progerin and lamin C bands on the immunoblot shown in Fig. 1e. The intensity of each band was normalized by α-tubulin intensity and compared to the normalized mock-control. **b**, Immunoblot of adult liver lysate from g1&2-treated (5×10^{11} genomic copies per viral preparation) heterozygous HGPS (Pro/+) with hemi- or homozygous Cas9 background showing that a single copy of Cas9 is sufficient. **c**–**e**, Deep sequencing was performed on liver and heart DNA to measure the level of in vivo indel formation by each gRNA. **c**, Scheme of the deep sequencing strategy. gLmna-1 and gLmna-2 target sites are denoted by red arrows. ¥ denotes HGPS mutation. PCR amplicons of deep sequencing are indicated by black curved arrows. The locations of the primers (Lmna F and Lmna R) used for the first round of nested-PCR are denoted by green arrows. Liver (**d**) and heart (**e**) DNA samples were collected from 2.5-month-old Cas9 mice that had been injected at P0 with either of the gRNA viruses (gLmna-1 or gLmna-2;1.5×10^{11} genomic copies per viral preparation), or with no virus. Treatment with one gRNA resulted in the presence of indels at their corresponding target sites rather than at the target site of the other gRNA. No indels were detected in the 'no injection' controls. Each treatment was evaluated in two independent in vivo experiments.

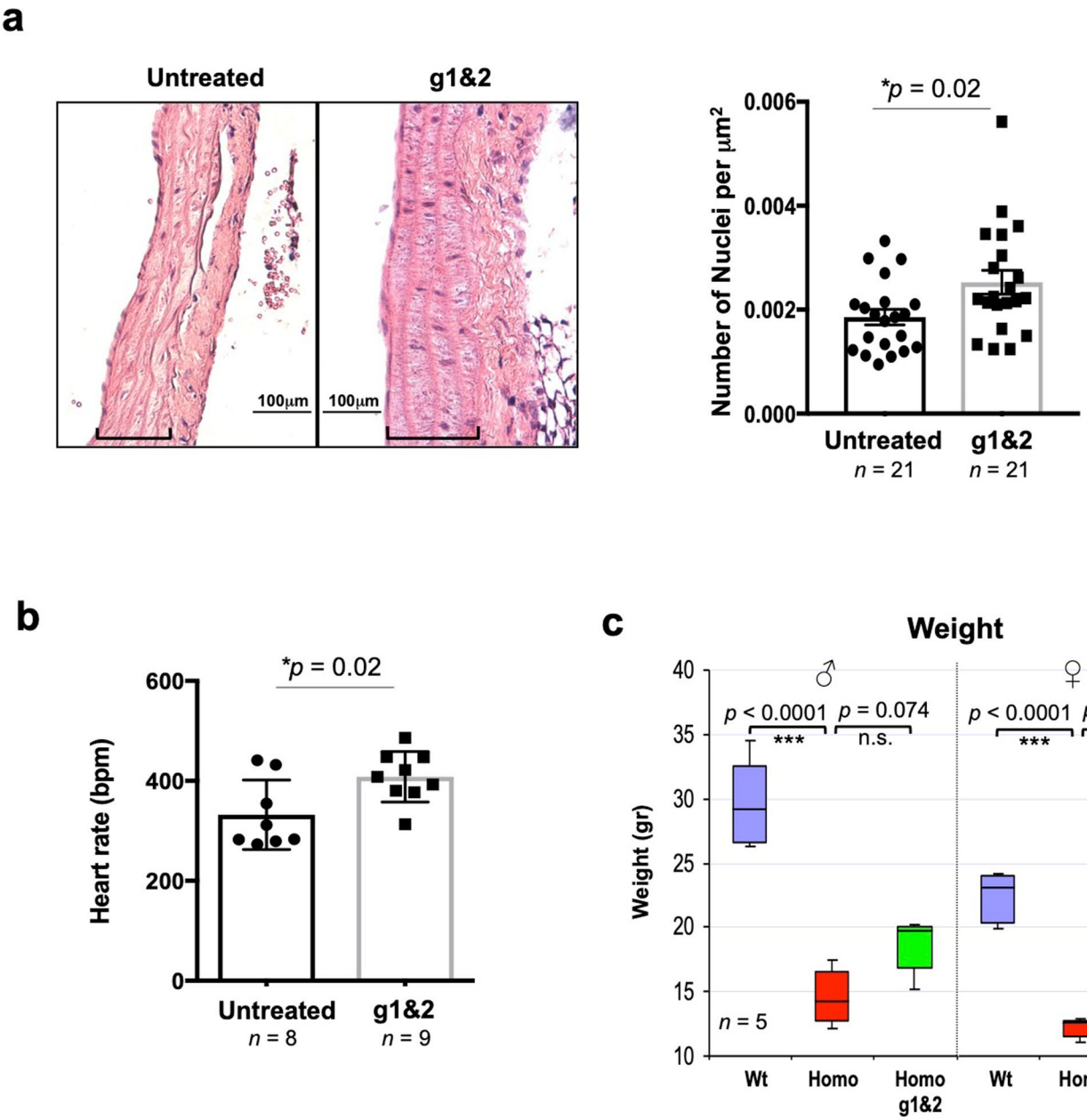

Extended Data Fig. 4 | Physiological analyses of Lmna gRNA-treated mice. a, Histological analysis of the aortic arch of untreated and gRNA-treated (g1&2) HGPS-Cas9 mice, 19 weeks old, injected at P0 with a 1:1 mix of gRNA1 and gRNA2 viral preparations. The black bracket shows the medial layer of the aortic arch. Scale bar, 100 μm. The bar graph on the right shows the number of nuclei in the medial layer ($n = 21$ for each group). **b**, Electrocardiographic analysis of untreated and gRNA-treated (g1&2) HGPS-Cas9 mice (untreated: $n = 8$; g1&2: $n = 9$). Heart rate is shown as beats per minute (bpm). **c**, Body weights of mice used for the grip strength test. Males and females are on the left and right, respectively. Cyan, red and green bars denote WT, negative control and treated mice, respectively. *P* values were calculated by unpaired Student's *t*-test. Data are presented as mean ± s.e.m. In each box plot, the box extends from the 25th to 75th percentiles and the black lines in the middle represent the median. The whiskers show the upper and lower limits of the range; significance was determined by one-way ANOVA with Bonferroni correction.

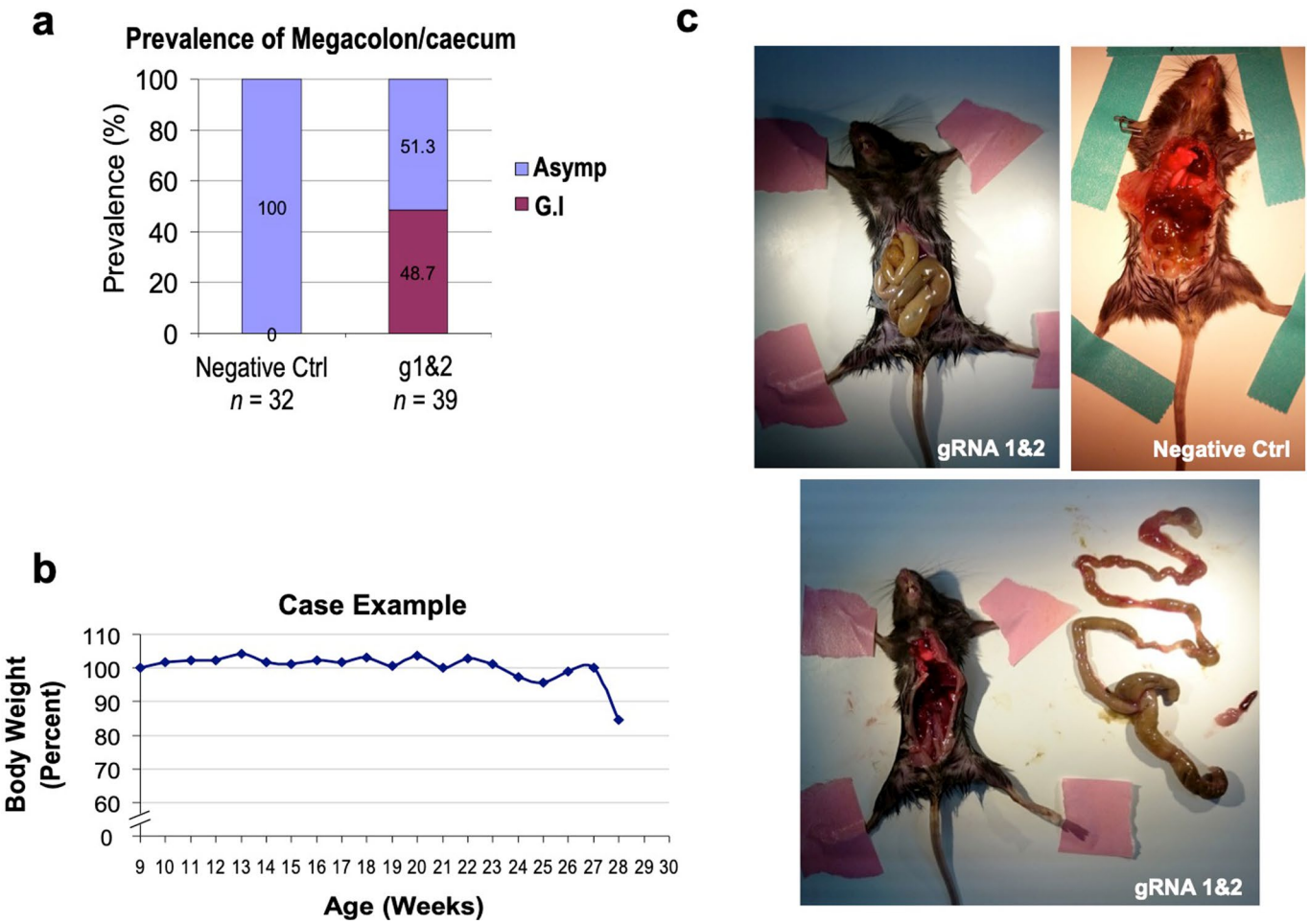

Extended Data Fig. 5 | Observed phenotypes of HGPS mice with extended lifespan. a, Prevalence of megacolon/megacecum among homozygous HGPS mice treated with gLmna-1 and 2 (g1&2) versus negative controls. Asymp: asymptomatic (no obvious gastrointestinal phenotype); G.I: gastrointestinal phenotype characterized by megacolon/megacecum and inability to defecate. **b**, Chenges in body weight of a representative g1&2-treated homozygous mouse that died suddenly after 28 weeks. **c**, Necropsy of a g1&2-treated homozygous mouse exhibiting megacolon/megacecum (left and bottom) versus negative control (right).

nature research

Corresponding author(s): Prof. Juan Carlos Izpisua Belmonte

Reporting Summary

Nature Research wishes to improve the reproducibility of the work that we publish. This form provides structure for consistency and transparency in reporting. For further information on Nature Research policies, see Authors & Referees and the Editorial Policy Checklist.

Statistical parameters

When statistical analyses are reported, confirm that the following items are present in the relevant location (e.g. figure legend, table legend, main text, or Methods section).

n/a	Confirmed	
☐	☒	The exact sample size (*n*) for each experimental group/condition, given as a discrete number and unit of measurement
☒	☐	An indication of whether measurements were taken from distinct samples or whether the same sample was measured repeatedly
☐	☒	The statistical test(s) used AND whether they are one- or two-sided *Only common tests should be described solely by name; describe more complex techniques in the Methods section.*
☐	☒	A description of all covariates tested
☐	☒	A description of any assumptions or corrections, such as tests of normality and adjustment for multiple comparisons
☐	☒	A full description of the statistics including central tendency (e.g. means) or other basic estimates (e.g. regression coefficient) AND variation (e.g. standard deviation) or associated estimates of uncertainty (e.g. confidence intervals)
☐	☒	For null hypothesis testing, the test statistic (e.g. *F*, *t*, *r*) with confidence intervals, effect sizes, degrees of freedom and *P* value noted *Give P values as exact values whenever suitable.*
☒	☐	For Bayesian analysis, information on the choice of priors and Markov chain Monte Carlo settings
☒	☐	For hierarchical and complex designs, identification of the appropriate level for tests and full reporting of outcomes
☒	☐	Estimates of effect sizes (e.g. Cohen's *d*, Pearson's *r*), indicating how they were calculated
☐	☒	Clearly defined error bars *State explicitly what error bars represent (e.g. SD, SE, CI)*

Our web collection on statistics for biologists may be useful.

Software and code

Policy information about availability of computer code

Data collection	No data collected from commercial, open source and custom code.
Data analysis	Microsoft Excel, GraphPad Prism7

For manuscripts utilizing custom algorithms or software that are central to the research but not yet described in published literature, software must be made available to editors/reviewers upon request. We strongly encourage code deposition in a community repository (e.g. GitHub). See the Nature Research guidelines for submitting code & software for further information.

Data

Policy information about availability of data

All manuscripts must include a data availability statement. This statement should provide the following information, where applicable:

- Accession codes, unique identifiers, or web links for publicly available datasets
- A list of figures that have associated raw data
- A description of any restrictions on data availability

Accession code: GEO (GSE122865) for the data in Supplementary Figure 1c and Supplementary Figure 1d

Field-specific reporting

Please select the best fit for your research. If you are not sure, read the appropriate sections before making your selection.

☒ Life sciences ☐ Behavioural & social sciences ☐ Ecological, evolutionary & environmental sciences

For a reference copy of the document with all sections, see nature.com/authors/policies/ReportingSummary-flat.pdf

Life sciences study design

All studies must disclose on these points even when the disclosure is negative.

Sample size	Sample size is indicated on the Figures. No statistical method was used to predetermine sample size. Sample size was chosen based on the sample availability and statistic relevance
Data exclusions	For the voluntary running wheel activity, the animals were allowed to adapt to the wheels for at least 22 hours before integrating their activity into the estimates. The activities were integrated in only after the mice became adjusted to the wheels as determined by the activities showing circadian correlation (active at night). One of the 27 analyzed mice showed no interest on the running wheels as determined by small sporadic peaks of activity with no circadian correlation. This mouse mouse was excluded from the study. All the mice that showed even low activity but with circadian correlation were included.
Replication	All statistic data are presented as mean ± standard deviation. All samples represent a minimum of two replicates. It has indicated in each figure legend.
Randomization	No randomization method was used. Animals and samples were randomly allocated into experimental groups.
Blinding	No blinding was performed. All animals were genotyped to confirm the transgenic background.

Reporting for specific materials, systems and methods

Materials & experimental systems

n/a	Involved in the study
☐	☒ Unique biological materials
☐	☒ Antibodies
☐	☒ Eukaryotic cell lines
☒	☐ Palaeontology
☐	☒ Animals and other organisms
☒	☐ Human research participants

Methods

n/a	Involved in the study
☒	☐ ChIP-seq
☒	☐ Flow cytometry
☒	☐ MRI-based neuroimaging

Unique biological materials

Policy information about availability of materials

Obtaining unique materials	No restrictions. All the materials used are available from the authors or commercial sources.

Antibodies

Antibodies used	The following antibodies were used for immunoblotting at the indicated dilution: Anti-LAMIN A/C (N-18) 1:100 (SantaCruz, Catalogue No: sc6215), Anti-LAMIN A/C (E-1) 1:100 (SantaCruz, Catalogue No: sc376248), anti-β actin 1: 600 (SantaCruz, Catalogue No: sc47778), anti-α tubulin 1: 750 (Calbiochem, Catalogue No: CP06). HRPconjugated secondary antibodies were anti-goat 1:500 (Novex, Catalogue No: A15909), anti-mouse 1:1000 (Cell Signaling, Catalogue No: 7076).
Validation	The antibodies were validated on the immunoblots based on the expected sizes of their corresponding antigens as assessed by protein marker ladders loaded on the gels. Lamin A/C antibodies were additionally confirmed by the comparison of the signal band patterns of HGPS homozygous versus heterozygous and wildtype lysates.

Eukaryotic cell lines

Policy information about cell lines

Cell line source(s)	Primary fibroblasts isolated from the tail tips of in-house mice of the indicated genotypes
Authentication	The genotypes were confirmed by PCR
Mycoplasma contamination	Period mycoplasma assays were performed in the lab and no contamination was detected.
Commonly misidentified lines (See ICLAC register)	No such cell line was used

Animals and other organisms

Policy information about studies involving animals; ARRIVE guidelines recommended for reporting animal research

Laboratory animals	The HGPS (Progeria) mouse model, carrying the progerin mutation G609G was generated by Carlos López-Otín at the University of Oviedo. Streptococcus pyogenes Cas9 transgenic mice were obtained from the Jackson Laboratory (Stock No: 024858). Homozygous Progeria mice are infertile. The heterozygous mice were crossed with homozygous Cas9 mice to obtain the composite mice. The resulting trans-heterozygous mice were bred to obtain the homozygous Progeria mice that carried the Cas9 transgene (homo or hemizygous). Hemizygous Cas9 mice did not significantly differ from the homozygotes in terms of the gene editing efficiency (Supp. Fig. 2c). The heterozygous Progeria mice on the Cas9 background were used to maintain the line. Progeria mice are C57BL/6 strain. Cas9 mice are on a mixed background of 129, C57BL/6 and FVB/N. The mice were housed with a 12 hours light/dark cycle between 06:00 and 18:00 in a temperature controlled room (22 ± 1°C) with free access to water valves and PicoLab Rodent Diet 20 (LabDiet, Catalogue No: 5053) provided on a wire bar lid. Mice that have lost more than 20% weight within a week, or those that fell below 13 gram were provided moist food on the cage floor and a water bottle on the wire bar lid. The age and sex of the mice are indicated in the corresponding figures. The mice were injected at P0-2 and continued to check the body weight and survival rate until week 32.
Wild animals	The study did not involve wild animals.
Field-collected samples	s The study did not involve samples collected from the field.